Characterization of polyurea microcapsules synthesized with an isocyanate of low toxicity and eco-friendly esters via microfluidics: Shape, shell thickness, morphology and encapsulation efficiency

Jiupeng Du, Nelson Ibaseta, Pierrette Guichardon

Characterization of polyurea microcapsules synthesized with an isocyanate of low toxicity and eco-friendly esters via microfluidics: Shape, shell thickness, morphology and encapsulation efficiency

Jiupeng Du, Nelson Ibaseta, Pierrette Guichardon *

Aix Marseille Univ, CNRS, Centrale Marseille, M2P2 Marseille, France

ARTICLE INFO

Article history:
Received 26 December 2021
Received in revised form 4 March 2022
Accepted 16 March 2022
Available online 26 March 2022

Keywords:
Microfluidics
Polyurea microcapsule
Amine concentration
Microcapsule deformation
Shell thickness
Morphology

ABSTRACT

There are some studies on the synthesis of polyurea microcapsules. However, there is hardly a case where both green solvents and non-toxic isocyanates are used, especially in microfluidics. In this work, an environmentally friendly chemical system of interfacial polymerization (isocyanate: HDB-LV; solvent: octyl salicylate or dibutyl adipate) is tested for the first time to produce polyurea microcapsules. The size of microcapsules is calibrated at 78 μm by microfluidics to quantitatively analyze the relationships among shell thickness, encapsulation efficiency and isocyanate concentrations. The influences of solvent types and reactant concentrations on the shape, morphology and shell thickness of microcapsules are studied. Esters with low water miscibility and low amine concentrations (lower reaction rate) are crucial for the formation of spherical microcapsules. An ester with high water miscibility can diffuse into the continuous phase during encapsulation, which results in broken microcapsules. A high concentration of amine can probably cause cross-linking not only at the interface but also inside the droplet template, which leads to microcapsule deformation. A linear relationship is observed between the shell thickness of microcapsules and the isocyanate concentration. Overall, a high encapsulation efficiency (more than 90%) for octyl salicylate is achieved with polyurea microcapsules.

1. Introduction

In general, the purposes of microencapsulation can be classified into two parts: either to release (Ina et al., 2016; Zhang et al., 2018,2019b; Fujiwara et al., 2019; Eriksson et al., 2020; Sui et al., 2021) or to protect (De Castro and Shchukin, 2015; Park et al., 2019; Shi et al., 2020; Chen et al., 2020; Wu et al., 2021) core materials. To protect or isolate core materials, hard and dense polymers should be used as shell materials. In the literature, typical satisfying polymers for protecting core materials are gelatin/gum Arabic complex (Onder et al., 2008; Shaddel et al., 2018), epoxy resin (Pascu et al., 2008), polymethyl methacrylate (Sari et al., 2009; Alkan et al., 2009), melamine resin (Chen et al., 2015; Sanchez-Silva et al., 2018; Zhang et al., 2020) and polyurea (Scarfato et al., 2007; Ji et al., 2010; Polenz et al., 2014).

The electrostatic bonding between gelatin and gum Arabic molecules determines that this complex material cannot provide enough protection for cores under certain conditions. High pH or high ionic strength can lead to dissociation of gelatin/gum Arabic complex (Tian et al., 2021; Muneratto

* Corresponding author.
E-mail address:
pierrette.guichardon@centrale-marseille.fr (P. Guichardon).

et al., 2021). Non-toxic epoxy resin microcapsules are first reported by Pascu et al. Pascu et al. (2008) and are considered as good candidates for protecting cores. Recently, epoxy resin is often used with melamine resin or polyurea to produce self-healing microcapsules (Cotting et al., 2019; Jialan et al., 2019; Tzavidi et al., 2020). However, the mechanical and chemical resistance of epoxy resin needs to be validated before it is further used as a protective shell material. Polymethyl methacrylate (PMMA) is regarded as an eco-friendly shell material for the fabrication of sealing microcapsules because of its low-cost (Sari et al., 2010) and non-toxicity (Ahangaran et al., 2019). But its moderate mechanical properties (Sari et al., 2010; Arora et al., 2010; Giro-Paloma et al., 2017) may need to be enhanced by surface modification for the usage as a protective polymer (Yang et al., 2015). In addition, a suitable initiator and a temperature around 80 °C are inevitable for polymerization of PMMA (Nandiyanto et al., 2012; Matamoros-Ambrocio et al., 2021). Melamine resin microcapsules exhibit good mechanical and chemical resistance as well as convenient synthesis conditions, so they are often used for enclosing fragrances (Fei et al., 2015; Leon et al., 2017; He et al., 2019) or phase-change materials (Sun et al., 2018; Yun et al., 2019) to achieve either retarding evaporation or energy storage, respectively. However, formaldehyde molecules are generally indispensable for the synthesis of melamine resin microcapsules. Unfortunately, the toxicity and volatility of formaldehyde can inevitably threaten environmental safety and present a significant risk to human health during the preparation of microcapsules. More seriously, the reactions for the synthesis of melamine resin are reversible, so the release of formaldehyde can potentially occur during the use of the microcapsules (Nguon et al., 2018).

In this case, polyurea, which has no known hazards and good mechanical and chemical properties, can be a good alternative (Valerie Jeanne-Rose, 2007; Zhang and Rochefort, 2012; Polenz et al., 2014). A classic process for microencapsulation by polyurea consists of two steps: an oil containing isocyanate molecules is first emulsified by a surfactant solution to form an oil-in-water (O/W) emulsion; in the next step, amine molecules are added into this emulsion to trigger the interfacial polymerization between isocyanates and amines.

Microcapsules with uniform size do not only pose more reproducible and controllable properties, but also simplify the analysis and modeling of results. Existing studies (Takahashi et al., 2007; Yang et al., 2013; Raeesi et al., 2017; Li et al., 2020; Njoku et al., 2020) on the relationships among shell thickness, isocyanates amount in droplet phases and encapsulation efficiency of polyurea microcapsules, are mostly conducted using a conventional emulsification method, where the size distribution is not negligible. Consequently, it is difficult to establish quantitative relationships between the microcapsule's properties and isocyanates concentrations. To achieve the production of microcapsules with a narrow size distribution, droplet microfluidics is considered as an efficient and promising technique to produce a monodispersed emulsion and thus monodispersed microcapsules (Liu et al., 2009; Perez et al., 2015; Luo et al., 2017). Indeed, there are also some studies on the preparation of monodispersed polyurea microcapsules calibrated via microfluidics. For example, (Polenz et al., 2014) investigate the influence of isocyanate and amine concentrations respectively on the shell thickness of polyurea microcapsules. Zhang et al. (2019a) perform a similar study, but with a different chemical system. Yang et al. (2020) investigate the influence of amine properties such as viscosity, polarity and reactivity on shell thickness of polyurea microcapsules. Lai et al. (2021) find that synthesis temperature also has an influence on shell formation. However, none of them uses a non-toxic chemical system for the preparation of monodispersed polyurea microcapsules using microfluidics.

In fact, isocyanate monomers such as TDI, HDI and IPDI are commonly used in existing studies to form polyurea microcapsules, as summarized in Table 1. These small isocyanate molecules have high reactivity but also high toxicity because they are highly volatile and harmful to humans and environment (Bulian and Graystone, 2009). Some polyisocyanates like HDB-LV (HDI biuret) have almost no volatility and are much safer to handle. To our best knowledge, there is no systematic study on the formation of monodispersed polyurea microcapsules with HDB-LV.

Besides, organic core liquids are used directly to dissolve isocyanates for the formation of polyurea microcapsules. However, in some cases, it is still necessary to use a co-solvent to dissolve isocyanates. For example, in order to encapsulate some phase-change materials (PCM) that have very limited miscibility with isocyanates, an organic co-solvent like cyclohexane is inevitable (Lu et al., 2017; Cai et al., 2020; Ma et al., 2012). Esters such as octyl salicylate and dibutyl adipate are much less toxic than cyclohexane, but to our best knowledge they are never reported in the literature for polyurea microcapsule formation. Moreover, our previous study (Du et al., 2020) has confirmed that these green esters can be successfully emulsified in a microchannel with the help of suitable surfactants. Therefore, it is time to verify the possibility of producing polyurea microcapsules for these two solvents. We hope that this work can also be used for studies dealing with energy storage applications through microcapsules.

Herein, we try to fabricate the polyurea microcapsules with a less toxic isocyanate (HDB-LV) and two eco-friendly esters (octyl salicylate and dibutyl adipate). Meanwhile, microfluidic emulsification is performed to calibrate the size of microcapsules. The main purposes of this work are to investigate the feasibility of producing polyurea microcapsules with such a new chemical system and to quantitatively indicate the relationships among shell thickness, encapsulation efficiency and isocyanate concentrations. First, we attempt to prepare microcapsules with a relatively high amine concentration in the aqueous phase, which is commonly used in other studies to facilitate rapid polyurea shell formation (Polenz et al., 2014; Cai et al., 2020; Polenz et al., 2015; Lu et al., 2017,2011). Then, we show that the shape of the octyl salicylate-loaded microcapsules can be modified by decreasing amine concentration, and we investigate the effects of two organic solvents on microcapsule formation. Finally, we characterize the properties such as shape, morphology, shell thickness and encapsulation

Table 1 – Chemical systems used for the formation of polyurea microcapsules and the envisaged applications in existing studies.

Isocyanate	Chemical and physical properties of isocyanate	Solvent	Toxicity of solvent	Application	Ref
		Dodecanol dodecanoate	Unknown	PCM	Cai et al. (2020)
		KMC oil[a]	Category 1[b]	–	Polenz et al. (2015)
TDI[c]	High reactivity, high toxicity, the possibility of being photo-oxidized	N-octadecane	Category 1	PCM	Lu et al. (2017)
		Butyl stearate	Not classified as dangerous	PCM	Lu et al. (2011)
		Pirimiphos-methyl	Category 1	Agriculture	He et al. (2018)
		Solvent free	–	Self-healing	Khun et al. (2014)
		Solvent free	–	Self-healing	Huang and Yang (2011)
HDI[d]	High reactivity, high toxicity	Lavender	Not classified as dangerous	Cotton Fabrics	Wang et al. (2019)
		Solvent free	–	Self-healing	Sun et al. (2015)
		Linseed oil	Not classified as dangerous	Self-healing	Wang and Zhou (2018)
		N-octadecane	Category 1	PCM	Lone et al. (2013)
		Dimethylformamide	Category 1–4	Self-healing	Liu et al. (2021)
IPDI[e]	High reactivity, high toxicity	Xylene	Category 1–4	Agriculture	Hedaoo et al. (2014)
		Butyl stearate	Not classified as dangerous	PCM	Sun et al. (2021)
		Asphalt rejuvenator	Category 2–3	Architecture	Ji et al. (2021)
Desmodur[f]		Fragrances	Not classified as dangerous	Cosmetics	Jacquemond et al. (2009)
Desmodur	Low reactivity, low toxicity	Sunflower oil	Not classified as dangerous	Smart coating	Di Credico et al. (2013)
PMDI[g]		Butyl acetate	Not classified as dangerous	Self-healing	Ma et al. (2017)

[a] Diisopropyl naphthalene isomer mixture.
[b] Toxicity categories: category 1 has the highest toxicity. Classification according to Regulation (EC) No 1272/2008.
[c] 2,4-Toluene diisocyanate.
[d] 1,6-Hexamethylene diisocyanate.
[e] Isophorone diisocyanate.
[f] Name for a series of aromatic and aliphatic polyisocyanates such as an uretidone, an isocyanate or a biuret.
[g] Polymeric diphenylmethane diisocyanayte.

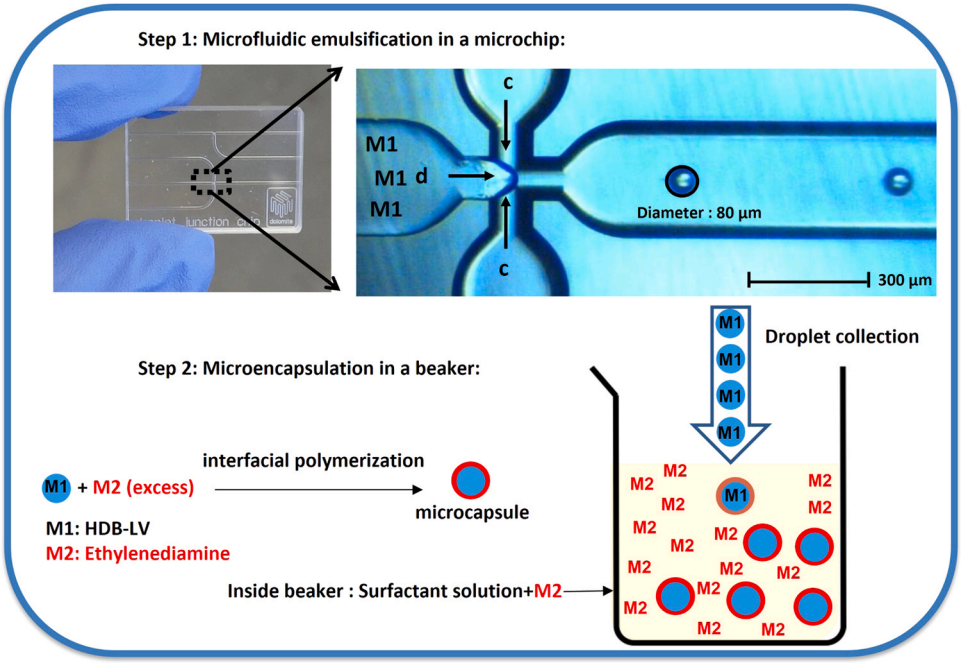

Fig. 1 – Schematic diagram of the experimental set-up for the production of polyurea microcapsules.

efficiency for the spherical microcapsules. Throughout the whole study, the size of microcapsules is calibrated at 78 μm with the help of microfluidics to avoid the size distribution effects on the above properties.

2. Materials and methods

2.1. *Materials*

The hexamethylene diisocyanate biuret (HDB-LV, Vencorex Chemicals, free isocyanate group in a molecule: 23.5 ± 1.0 wt %) is purchased from Vencorex. Sodium dodecyl sulfate (Across Organics, grade pure); ethylenediamine (Sigma Aldrich, ≥99%); octyl salicylate (or 2-ethylhexyl salicylate, Sigma Aldrich, ≥99%); dibutyl adipate (TCI, 99.9%); and 2-propanol (Sigma Aldrich, ≥99.9%) are used without additional purification. Distilled water is produced by mono-distillate 2008, GFL. All liquids are filtered through syringe filters (JVLAB, PTFE with 0.45 μm pore size) before being fed into the microchannel.

2.2. *Preparation of monodispersed polyurea microcapsules*

The polyurea microcapsules are prepared by a two-step process, as illustrated in Fig. 1. First, octyl salicylate (OS) or dibutyl adipate (DA) containing varying amounts of HDB-LV is emulsified (**Step 1** in Fig. 1) by a 1 wt% sodium dodecyl sulfate (SDS) solution in a hydrophilic flow-focusing microchip (Droplet Junction Chip, Dolomite Microfluidics ©, UK). Detailed information about the microfluidic set-up can be found in our previous study (Du et al., 2020). For different chemical systems of this study, the flow rates for dispersed (Q_d) and continuous phases (Q_c) are 2–4 μL/min and 107–138 μL/min respectively, to maintain droplet size at 78 μm.

In the next step, roughly 0.1 g (estimated by the flow rates of dispersed phases) of produced droplets are collected in a beaker (**Step 2** in Fig. 1) that contains one litre of an aqueous solution with 1 wt% SDS and 0.01–1 wt% Ethylenediamine (En). Then droplet collection is stopped and interfacial polymerization continues for four days at room temperature in the beaker. The molar amount of En (**M2**) in the beaker is roughly ten times higher than that of isocyanate groups (**M1**) within the collected droplets.

To investigate the influence of solvents, isocyanate (c_{HDB}) and amine (c_{En}) concentrations on the formation of polyurea microcapsules, different chemical systems are tested. Meanwhile, the size of droplets (or microcapsules) is maintained at 78 μm via microfluidics by adjusting the flow rates of dispersed and continuous phases. The different experimental sets are summarized in the Table 2.

2.3. *Characterization of microcapsules*

An optic microscope (model: AmScope BS200) with an integrated CMOS digital camera (MU 1803) is used to visualize droplets and microcapsules. The commercial AmScope software is available to measure the size of a single microcapsule manually. However, this local measurement is not very efficient for analyzing the size distribution of microcapsules because a sufficient number of microcapsules must be measured in one image to obtain reliable results. Hence, we develop a Matlab code to analyze size information of microcapsules from the optical micrographs. The principles for image processing via Matlab can be found in the supplementary material. A Scanning Electron Microscope (SEM, model: Philips XL30) is used to characterize the morphology and shell thickness of microcapsules. Microcapsules are washed by distilled water, dried in air and metalized by gold before the SEM characterization (Detailed method of SEM analysis is provided in supplementary material).

Encapsulation efficiency (EE %) is defined by the detected concentration (c_m) of core materials over its theoretical concentration (c_t) in microcapsules. Hence, EE % is calculated as below:

$$EE\% = \frac{c_m}{c_t} \times 100\%. \quad (1)$$

Table 2 – Table of experimental sets for the formation of polyurea microcapsules.

Num	Q_d, μL/min	Q_c, μL/min	C_{HDB}, wt%, wt%	C_{En}, wt%	Solvent	Continuous phase
set 1	2.0	138	30	1	OS	Unsaturated by OS
set 2	2.5	107	30	1	DA	Unsaturated by DA
set 3	2.0	138	30	1	OS	Saturated by OS
set 4	2.5	107	30	1	DA	Saturated by DA
set 5	3.1	117	10	1	OS	Unsaturated by OS
set 6	3.9	117	5	1	OS	Unsaturated by OS
set 7	2.0	138	30	0.5	OS	Unsaturated by OS
set 8	2.0	138	30	0.1	OS	Unsaturated by OS
set 9	2.0	138	30	0.05	OS	Unsaturated by OS
set 10	2.0	138	30	0.01	OS	Unsaturated by OS
set 11	2.5	107	30	0.01	DA	Unsaturated by DA
set 12	2.6	117	20	0.01	OS	Unsaturated by OS
set 13	3.1	117	10	0.01	OS	Unsaturated by OS
set 14	3.9	117	5	0.01	OS	Unsaturated by OS

To characterize encapsulation efficiency, approximately 0.05 g (controlled by an analytical balance: OHAUS PA214) of dry microcapsules loaded with OS are crushed in a mortar. The released OS as well as the crushed microcapsules are transferred to a flask. Then the mortar is washed with 30 ml of 2-propanol which is also transferred to the flask. In the end, 10 ml of supernatant is taken and diluted with 90 ml of 2-propanol. The amount of OS in this solution is measured using a UV Spectrophotometer (model: Cary 60) at its maximum absorbance peak of 307 nm. (Kim et al., 2001).

To obtain a simplified model for predicting the shell thickness, the density of droplets phases and of polyurea shells should be known. The two densities are measured with a densimeter (model: Anton Paar DMA 35) and a helium pycnometer (Quantachrome Instruments, model: Stereopycnometer), respectively.

3. Results

3.1. *Deformation of polyurea microcapsules for 1 wt% En*

From the related studies on the synthesis of polyurea microcapsules, the amine concentration in the aqueous phase is about 1–3 wt%. However, our first results show that the produced polyurea microcapsules are deformed when the amine concentration is 1 wt%, regardless of the solvent used.

3.1.1. *Influence of solvents on formation of polyurea microcapsules*

The microcapsules are prepared using OS and DA as solvent respectively, where the c_{HDB} is fixed at 30 wt%. The optical micrographs of the formed microcapsules are shown in Fig. 2. For both solvents used, the droplets (Fig. 2a) generated via the microfluidics are spherical and monodispersed with a size of 78 *μm*. However, the microcapsules are all deformed after polymerization when either OS (Fig. 2b) or DA (Fig. 2c) is used as the solvent. It can be seen that large ravines appear on the surface of microcapsules and this deformation of microcapsules is asymmetric.

Some studies (Jerri et al., 2016; Lei et al., 2019) show that diffusion of solvents into aqueous phases may cause deformation of microcapsules. To verify this, microcapsules are fabricated with the aqueous phases that are saturated with OS and DA respectively, while the other conditions remain unchanged. The formed microcapsules for saturated aqueous phases are presented in Fig. 2d and e for OS and DA, respectively. No obvious improvement is observed in the deformation of microcapsules.

3.1.2. *Influence of HDB-LV concentration on formation of polyurea microcapsules*

The other two HDB-LV concentrations (10 wt% and 5 wt%) are also tested for the synthesis of microcapsules when OS is used as solvent and 1 wt% En is used in the aqueous phase. Interestingly, with the decrease of c_{HDB}, the microcapsules deform less, as shown in Fig. 3. Spherical polyurea microcapsules (Fig. 3b) are eventually obtained when the c_{HDB} is 5 wt%. This phenomenon may indicate that the deformation of microcapsules at higher c_{HDB} may be due to a fast reaction rate.

3.2. *Influence of amine concentration on formation of polyurea microcapsules*

To verify if the reaction rate is the main reason leading to the deformation, microcapsules are produced by using different amine concentrations. We first use OS with 30 wt% of HDB-LV as the droplet phase. For different c_{En} in the aqueous phase, formed microcapsules are deposited on a glass slide and observed continuously by an optical microscope. The captured photos are shown in Fig. 4. When the c_{En} is too high ($\geq$ 0.5 wt%), microcapsules have obvious deformation within 10 min. The microcapsules begin losing their sphericity after five minutes for the highest c_{En} (1 wt%) used in this study. For lower c_{En} ($\leq$ 0.1 wt%), there is no obvious change for the shape of microcapsules within 10 min

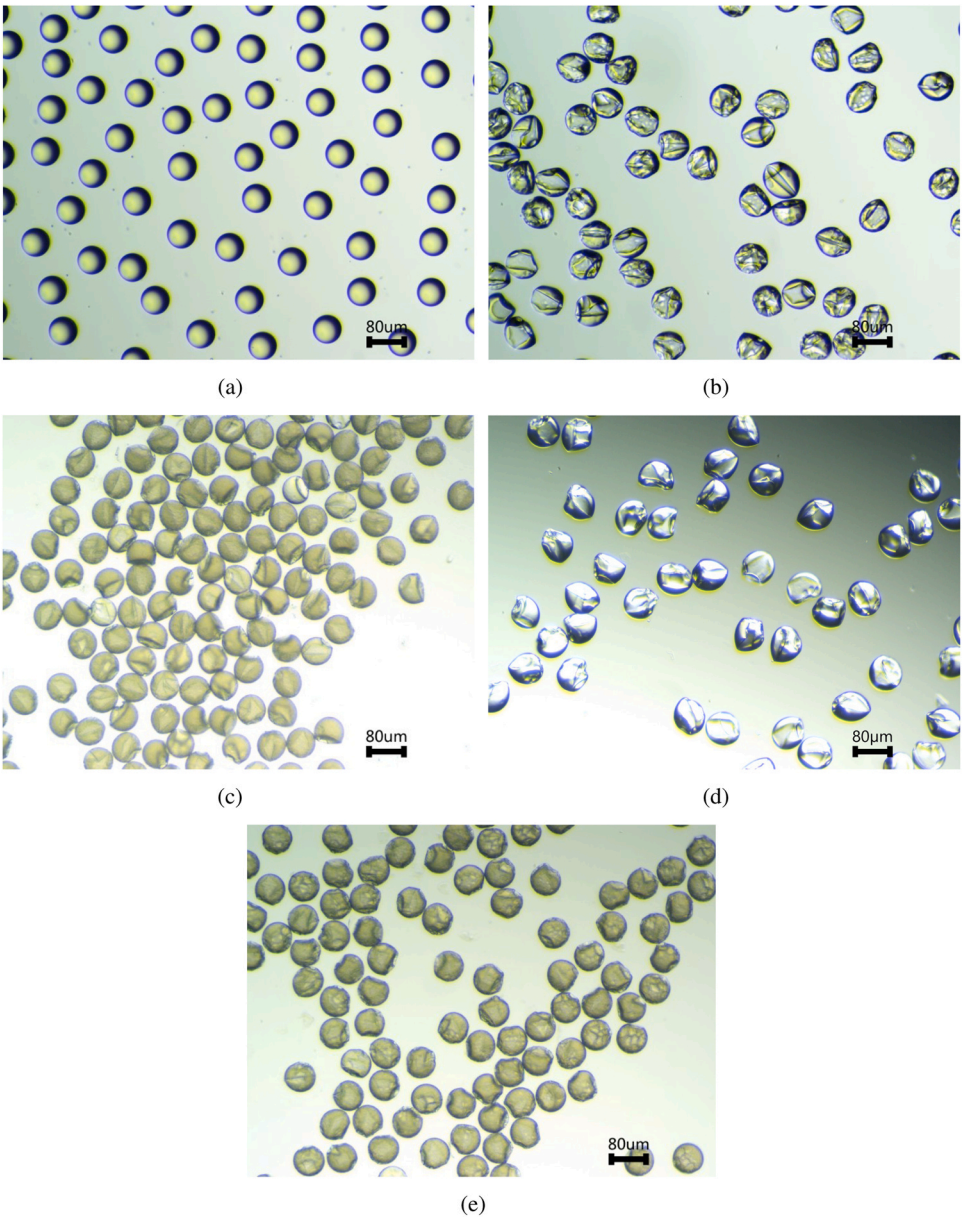

Fig. 2 – Deformation of the polyurea microcapsules for using different solvents where the c_{HDB} and c_{En} are fixed at 30 wt% and 1 wt%, respectively. (a). Droplets of 78 *μm*. (b). OS is used as the solvent and the aqueous phase is not saturated by OS. Operating condition: set 1. (c). DA is used as the solvent and the aqueous phase is not saturated by DA. Operating condition: set 2. (d). OS is used as the solvent and the aqueous phase is saturated by OS. Operating condition: set 3. (e). DA is used as the solvent and the aqueous phase is saturated by DA. Operating condition: set 4.

However, after four days of reaction in a beaker, only the microcapsules synthesized under 0.01 wt% c_{En} are not deformed, as shown in Fig. 5. Although some slight craters appear on the surface of microcapsules at this amine concentration, the microcapsules (Fig. 5a) are globally spherical compared to the those (Fig. 5b-d) synthesized under higher c_{En} (≥ 0.05 wt%).

Then DA with 30 wt% of HDB-LV is also tested as the droplet phase to fabricate microcapsules when c_{En} is fixed at 0.01 wt%. The formed microcapsules are all broken and with very various sizes after the polymerization, as shown in Fig. 5e. This is caused by the relatively high solubility (35 mg/L) of DA in the aqueous phase. Whereas, OS has a much smaller solubility (0.6206 mg/L) in the aqueous phase and thus almost no diffusion happens during the formation of microcapsules.

Given the results above, the optimal c_{En} is determined to be 0.01 wt%. And OS is chosen to be the core liquid to produce spherical polyurea microcapsules. These spherical microcapsules are characterized for their sizes, morphology, shell thickness and encapsulation efficiency in the next.

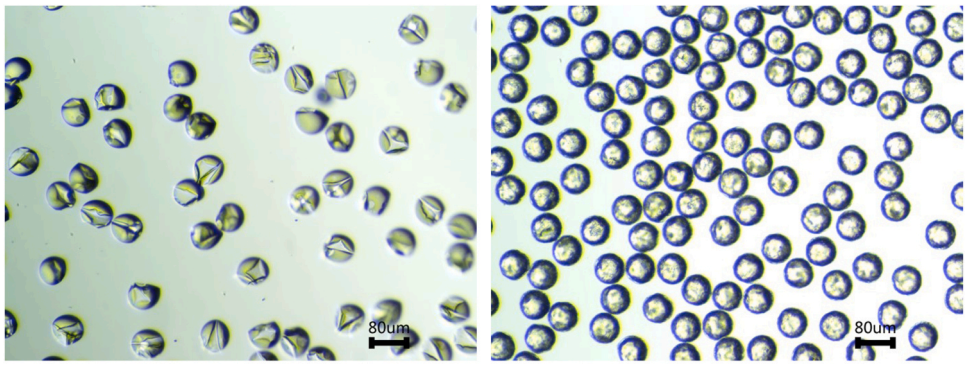

Fig. 3 – Deformation of the polyurea microcapsules at different c_{HDB} when OS is used as the solvent and c_{En} is fixed at 1 wt%. (a). The microcapsules for the c_{HDB} at 10 wt%. Operating condition: set 5. (b). The microcapsules for the c_{HDB} at 5 wt%. Operating condition: set 6.

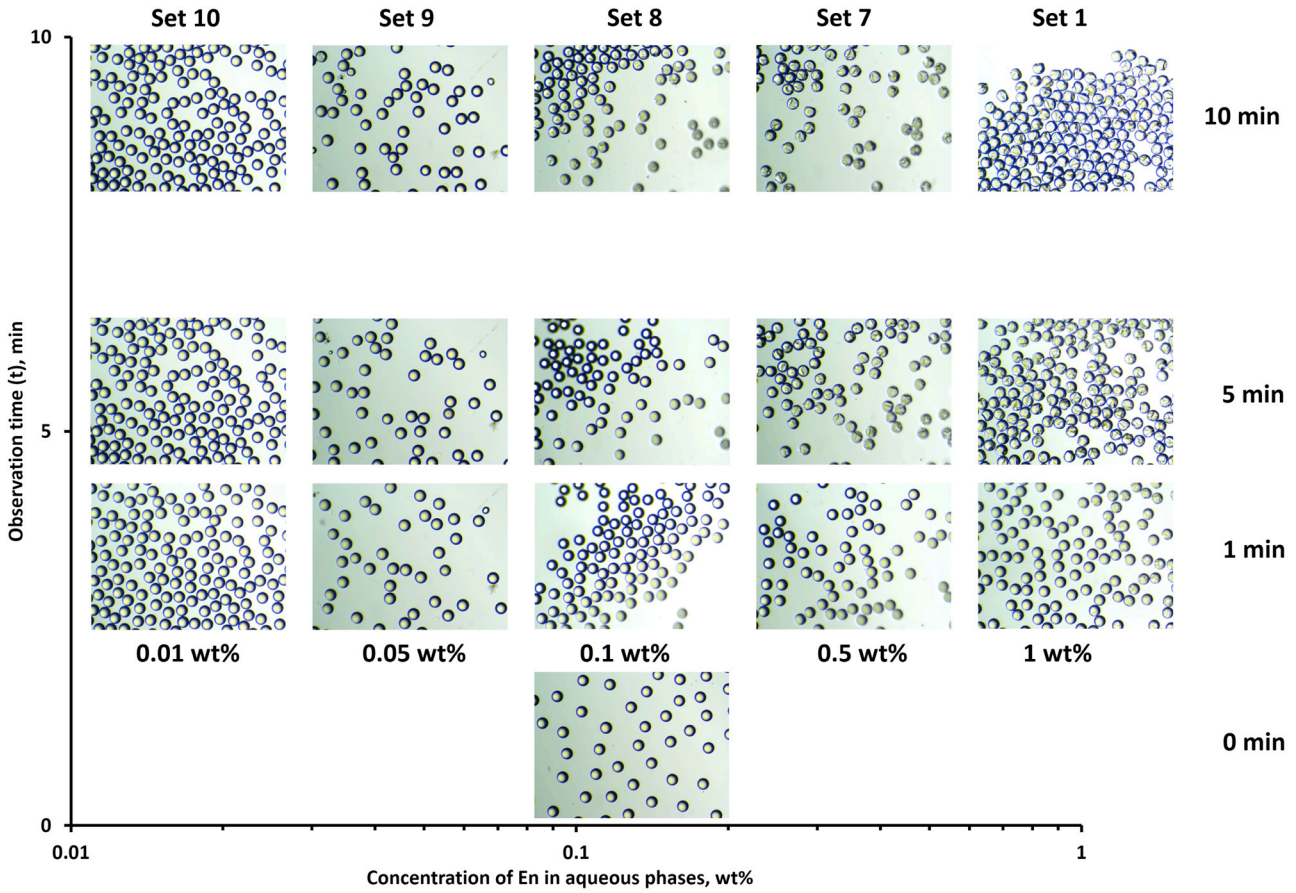

Fig. 4 – A ten-minute evolution of the microcapsules' shape with time at different c_{En}. The mass ratio of the OS/HDB-LV is fixed at 7:3 for all chemical systems. Photos are captured for the droplets that are deposited on glass slides. The corresponding experiment sets are as follows: set 1, 7, 8, 9 and 10.

3.3. *Size of droplets and microcapsules*

3.3.1. *Size of droplets and microcapsules synthesized at different conditions*

Micrographs of droplets and the microcapsules synthesized with 30 wt% of c_{HDB} are given as an example to explain the image processing for their size information, as illustrated in Fig. 6. Although the microcapsules have rough surfaces with some craters, they are monodispersed without apparent change in size. To analyse efficiently size information for droplets and microcapsules, image processing via Matlab is developed, as illustrated in Fig. 6a and b. The coefficients of variation (CV) of sizes are calculated by Eq. (2) to be 1.0% and 1.8% for the droplets and microcapsules, respectively.

$$CV = \frac{\sigma}{\bar{d}} \tag{2}$$

Where σ is the standard deviation of droplet diameter and $\bar{d}$ is the mean droplet diameter. Micrographs for the microcapsules synthesized with the c_{HDB} at 20 wt%, 10 wt%, and 5 wt% respectively can be found in the supplementary material (Fig. S6).

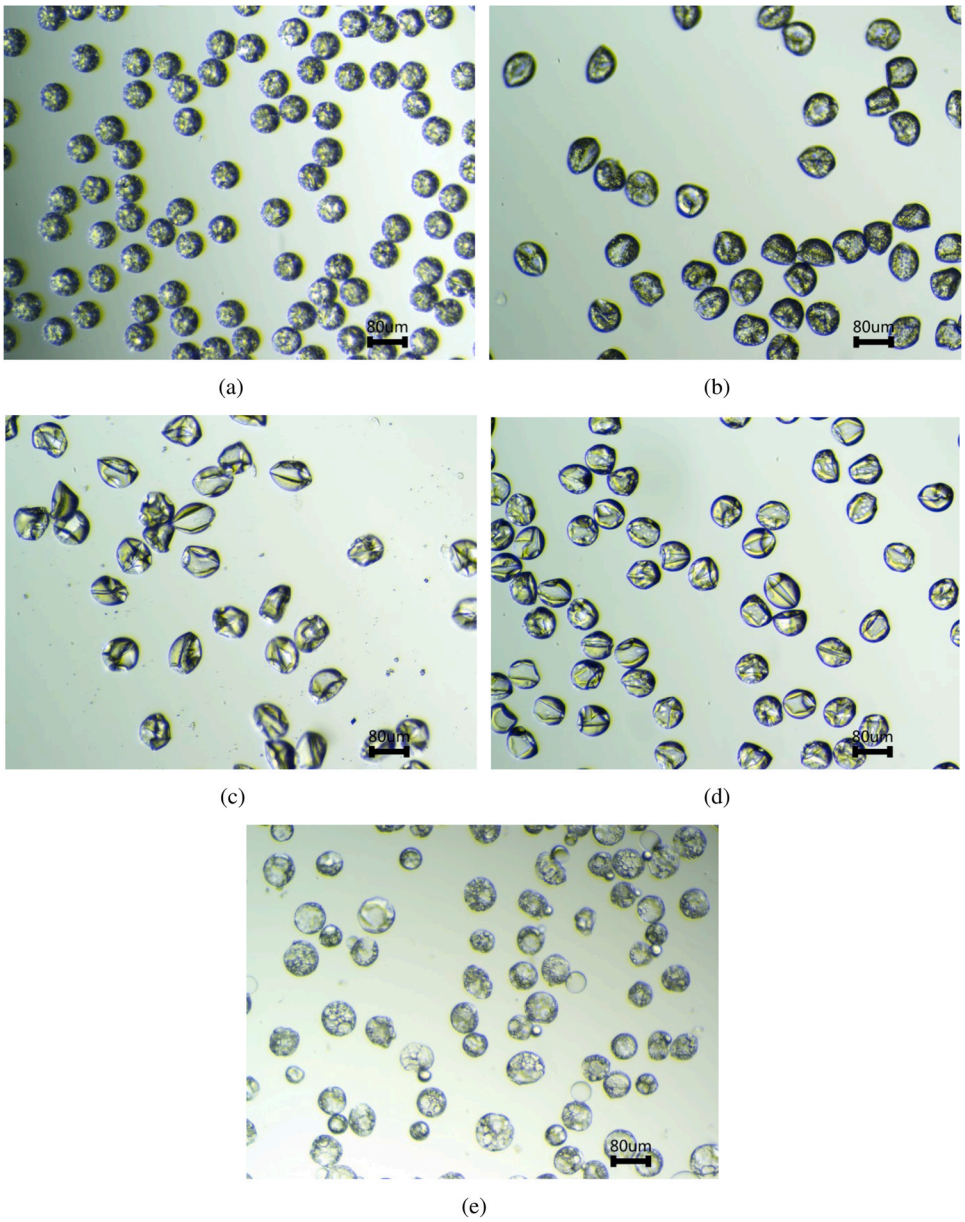

Fig. 5 – Deformation of the polyurea microcapsules at different c_{En} after four days polymerization. (a). The microcapsules for the c_{En} at 0.01 wt% and c_{HDB} at 30 wt%. Operating condition: set 10. (b). The microcapsules for the c_{En} at 0.05 wt% and c_{HDB} at 30 wt%. Operating condition: set 9. (c). The microcapsules for the c_{En} at 0.1 wt% and c_{HDB} at 30 wt%. Operating condition: set 8. (d). The microcapsules for the c_{En} at 1 wt% and c_{HDB} at 30 wt%. Operating condition: set 1. (e). The microcapsules for the c_{En} at 0.01 wt% and c_{HDB} at 30 wt%. Operating condition: set 11.

The sizes of droplets and microcapsules synthesized with different c_{HDB} are summarized in Table 3. In general, the polyurea shells grow towards the inside direction of the microcapsules. However, droplet sizes are slightly smaller than those of the corresponding microcapsules with a difference of less than 3.2%. Because microcapsules have rough surfaces on which there are many craters, this difference is probably caused by measurement errors. In the following parts of this study, the external diameters of microcapsules can be reasonably considered as the same as the size of droplets to simplify calculations.

The information of flow rates for the corresponding experimental sets can be read from Table 2. For the dispersed phase with 30 wt% of c_{HDB}, the microcapsules with an average size of 78 μm are fabricated at the Q_c of 138 μL/min and the Q_d of 2.0 μL/min. To remain droplet sizes at around 78 μm for different c_{HDB} (from 5 to 20 wt%), different Q_d should be used if the Q_c is fixed at 117 μL/min. Q_d decreases with an increase of c_{HDB} because the dispersed phase is more viscous at a higher c_{HDB}.

3.4. *Morphology and shell thickness of the microcapsules*

3.4.1. *Morphology of the microcapsules under different synthesis conditions*

The SEM photos of polyurea microcapsules (78 μm) for different c_{HDB} from 5 wt% to 30 wt% are shown in Fig. 7a-d. The obtained microcapsules are monodispersed and globally

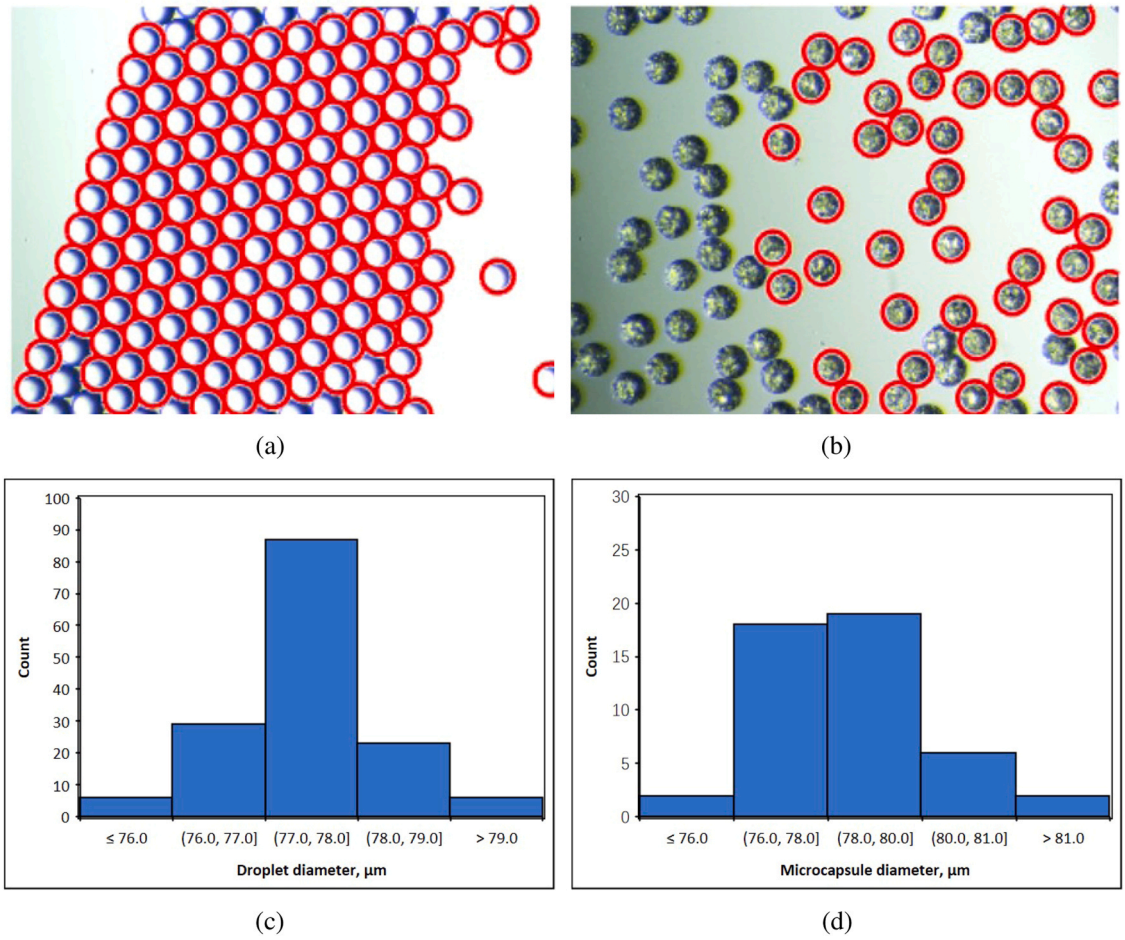

Fig. 6 – Image processing for the droplets and polyurea microcapsules synthesized with 30 wt% of c_{HDB}. Operating condition: set 10. (a) and (b) are the micrographs in which the spherical droplets and microcapsules are identified respectively, after the image processing via a Matlab code. (c) and (d) are size distribution histograms for the droplets and microcapsules respectively.

Table 3 – The sizes of microcapsules synthesized at different conditions.

Num	c_{HDB}, wt %, wt%	Droplet size, μm	Capsule size, μm	CV of capsule size
Set 10	30	77.5 ± 0.8	78.5 ± 1.5	1.8%
Set 12	20	77.0 ± 0.9	78.6 ± 1.8	2.3%
Set 13	10	76.5 ± 0.8	78.1 ± 1.0	1.4%
Set 14	5	77.2 ± 1.7	78.8 ± 1.2	1.5%

spherical although some craters appear on their surface, which is consistent well with the observation by the optical microscope. Besides, the obtained microcapsules are not porous because there is no obvious hole on the surface.

When c_{HDB} is at or over 20 wt%, the obtained microcapsules are well dispersed as shown in Fig. 7a and b, respectively. However, with the decrease of c_{HDB}, the formed microcapsules tend to stick together (Fig. 7c) and even merge like a honeycomb (Fig. 7d). There are possible two reasons for this phenomenon. When the quantity of the HDB-LV in the droplet is not enough, the formed shells are so fragile that the core material is not completely isolated by the shell. Hence, once these microcapsules are washed by distilled water and dried, they tend to gather to reduce their total interfacial energy (Fujiwara et al., 2020). Besides, a high vacuum environment (10^{-5} mbar) inside the SEM may cause volume expansion of the encapsulated OS. And this expansion can destroy the shells, which eventually causes the merging of those microcapsules.

3.4.2. *Shell thickness of the microcapsules under different synthesis conditions*

The shell thicknesses (β) of microcapsules (78 μm) at different c_{HDB} are shown in Fig. 8a–d. Shell thicknesses and sizes of microcapsules that are characterized by SEM are summarized in Table 4. With the increase of c_{HDB}, the shells of microcapsules get thicker. A linear relationship between c_{HDB} and shell thickness of microcapsules is found, as shown in Fig. 9.

3.5. *Encapsulation efficiency (EE %)*

3.5.1. *Standard UV absorbance curve for the octyl salicylate in 2-propanol*

The absorbance at the wavelength of 307 nm is chosen for the quantification of OS in 2-propanol solutions. A standard absorbance curve at 307 nm for OS with different concentrations in 2-propanol is obtained and shown in Fig. 10. The mass extinction coefficient of OS is 20.2 $L \cdot g^{-1} \cdot cm^{-1}$, which is consistent well with that (20.0 $L \cdot g^{-1} \cdot cm^{-1}$) in the literature (Kim et al., 2001). The molar extinction coefficient is calculated to be $5.05 \times 10^3 L \cdot mol^{-1} \cdot cm^{-1}$.

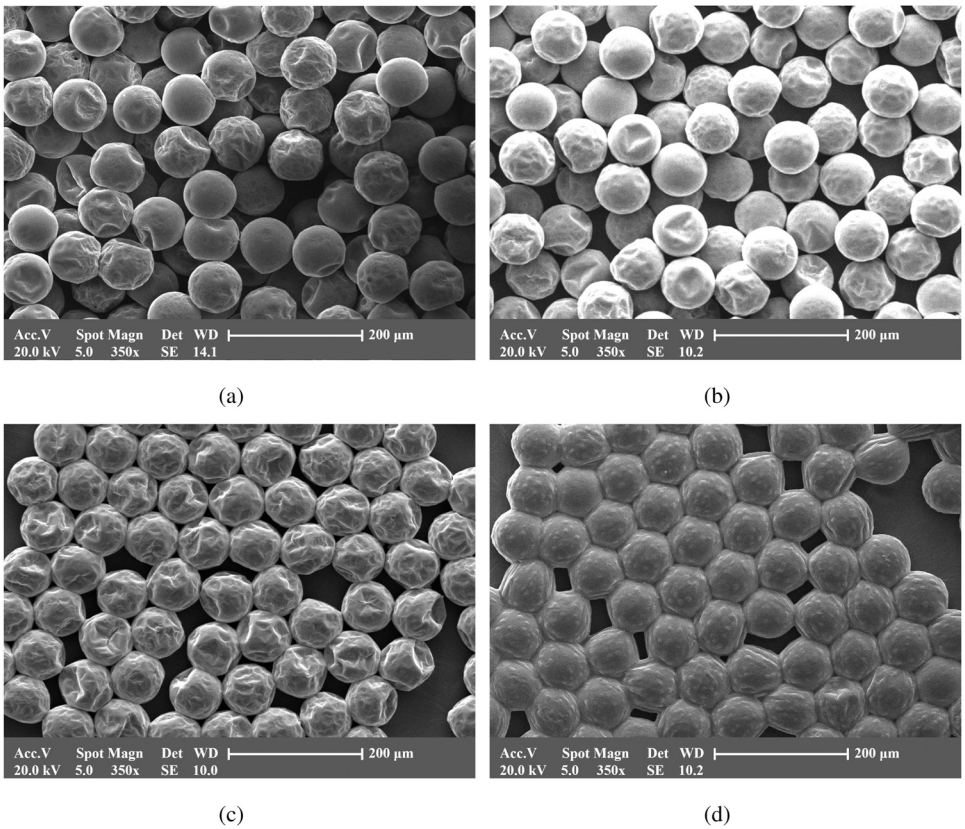

Fig. 7 – SEM photos of the polyurea microcapsules synthesized with different c_{HDB}. (a). c_{HDB} at 30 wt%. Operating condition: set 10. (b). c_{HDB} at 20 wt%. Operating condition: set 12. (c). c_{HDB} at 10 wt%. Operating condition: set 13. (d). c_{HDB} at 5 wt%. Operating condition: set 14.

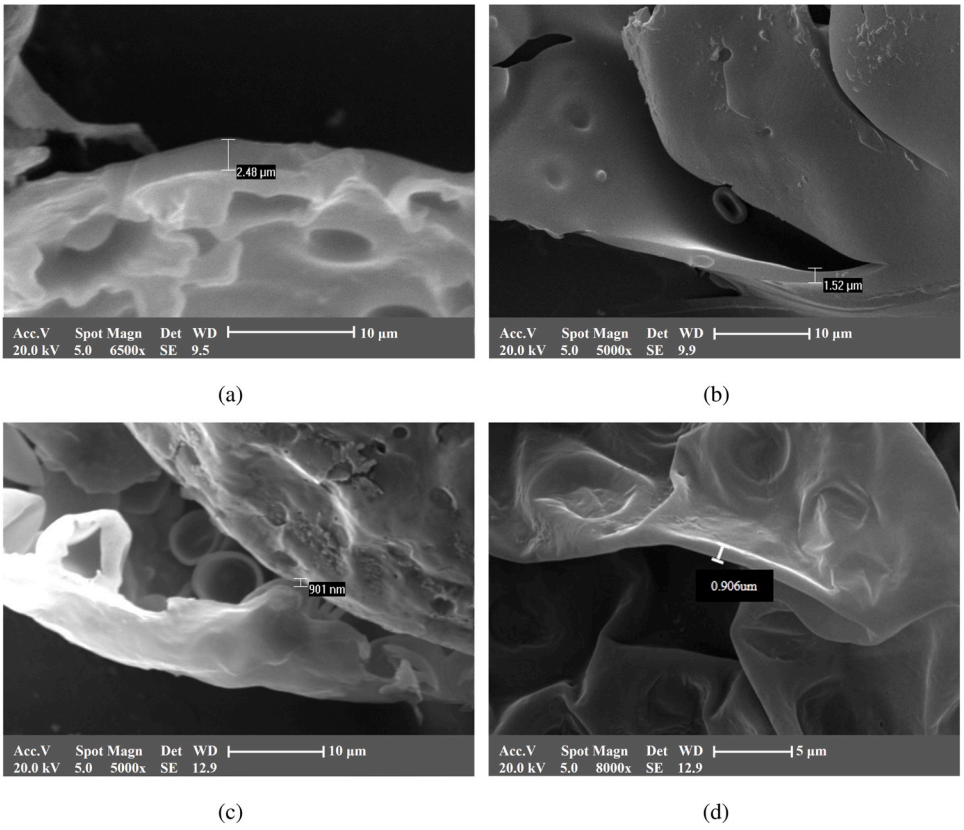

Fig. 8 – The shell thickness of the formed polyurea microcapsules synthesized with different c_{HDB}. (a). c_{HDB} at 30 wt%. Operating condition: set 10. (b). c_{HDB} at 20 wt%. Operating condition: set 12. (c). c_{HDB} at 10 wt%. Operating condition: set 13. (d). c_{HDB} at 5 wt%. Operating condition: set 14.

Table 4 – Shell thicknesses and sizes of microcapsules synthesized at different conditions characterized by SEM.

Num	c_{HDB}, wt%, wt%	Capsule size, μm	Shell thickness, μm
Set 10	30	78.4 ± 1.4	2.5 ± 0.3
Set 12	20	78.6 ± 1.0	1.5 ± 0.1
Set 13	10	79.2 ± 1.3	1.0 ± 0.1
Set 14	5	78.8 ± 1.6	0.4 ± 0.1

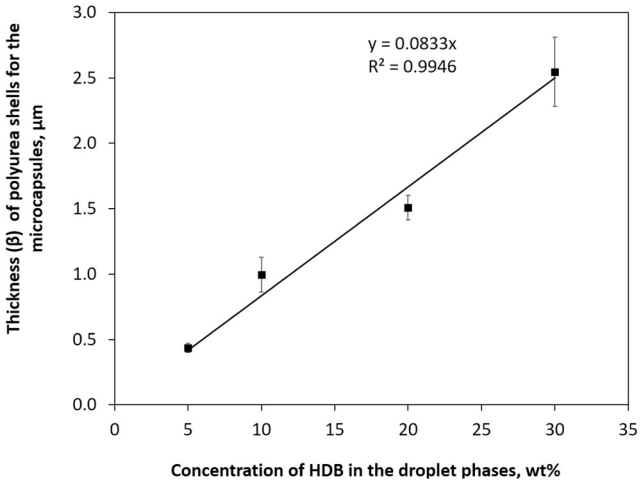

Fig. 9 – Shell thickness of microcapsules synthesized with different c_{HDB}. Size of the microcapsules: 78 μm.

3.5.2. *Encapsulation efficiency of the microcapsules under different synthesis conditions*

During interfacial polymerization, there are ethylenediamine (En) molecules that contribute also to the formation of polyurea shells. Therefore, the mass ratio of formed polyurea shells to OS cores should be calculated first. An example of calculating the theoretical concentration (c_t) is given as below for the microcapsules that are fabricated with a c_{HDB} of 30 wt%:

1) For m grams of the HDB-LV, the mass of the reacted En molecules is given as,

$$\frac{0.235m \times 60}{42 \times 2} = 0.17m \tag{3}$$

where the 0.235 is the mass percentage of free isocyanate groups in an HDB-LV molecule, 60 (g/mol) is the molar mass of En, 42 (g/mol) is the molar mass of isocyanate group and 2 is the number of amino groups in an amine molecule. For microcapsules fabricated with the c_{HDB} of 30 wt%, the mass percentage of OS in the microcapsule is calculated as,

$$\frac{7m}{3m + 7m + 0.17m \times 3} = 67\% \tag{4}$$

2) Thus, given 71 mg of these microcapsules, the theoretical mass of OS is calculated to be 48 *mg*.

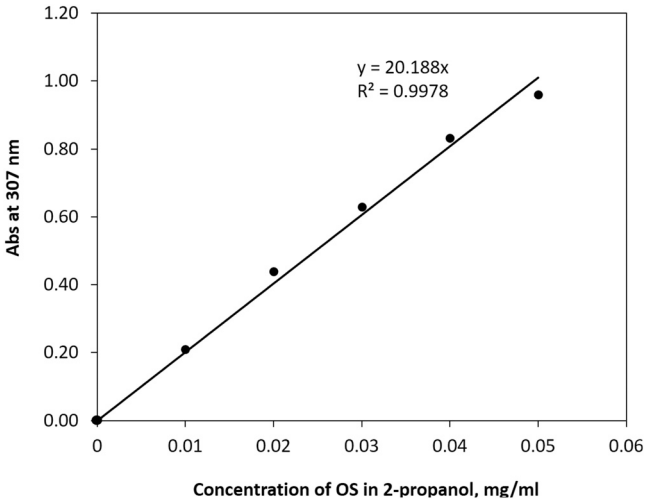

Fig. 10 – Standard curve of the UV absorbance at the wavelength of 307 nm for OS with different concentrations.

Table 5 – c_t values for the OS in synthesized polyurea microcapsules. a, b and c are different repetitions for the same experimental set.

Num	c_{HDB}, wt %, wt%	Crushed capsules, mg	2-Propanol used, ml	c_t, mg/ml
Set 10 a	30	71	1000	0.048
Set 10 b	30	71	1000	0.048
Set 12 a	20	61	1000	0.047
Set 12 b	20	63	1000	0.049
Set 13 a	10	52	1000	0.046
Set 13 b	10	52	1000	0.046
Set 14 a	5	52	1000	0.049
Set 14 b	5	52	1000	0.049
Set 14c	5	41	1000	0.039

3) If the above OS is diluted by 1000 ml of 2-propanol, the c_t is calculated to be 0.048 *mg/ml* by stoichiometry.c_t values for the OS in synthesized microcapsules are summarized in Table 5. The microcapsules with different chemical compositions are characterized at least twice.

The measured UV absorbance at the wavelength of 307 nm for different sample solutions are summarized in Table 6. The measured concentration (c_m) for OS is obtained according to the linear relationship (Abs = 20.188 c_m), as illustrated in Fig. 10. Finally, the encapsulation efficiency (EE %) is calculated as a ratio of c_m to c_t.

Table 6 – The c_m values for the OS in the microcapsules characterized in this study.

Num	Measured UV Abs	c_m, mg/ml	EE % (c_m/c_t × %)
Set 10 a	0.936	0.046	97%
Set 10 b	0.944	0.047	98%
Set 12 a	0.924	0.046	97%
Set 12 b	0.950	0.047	96%
Set 13 a	0.889	0.044	95%
Set 13 b	0.906	0.045	97%
Set 14 a	0.954	0.047	97%
Set 14 b	0.895	0.044	91%
Set 14c	0.702	0.035	90%

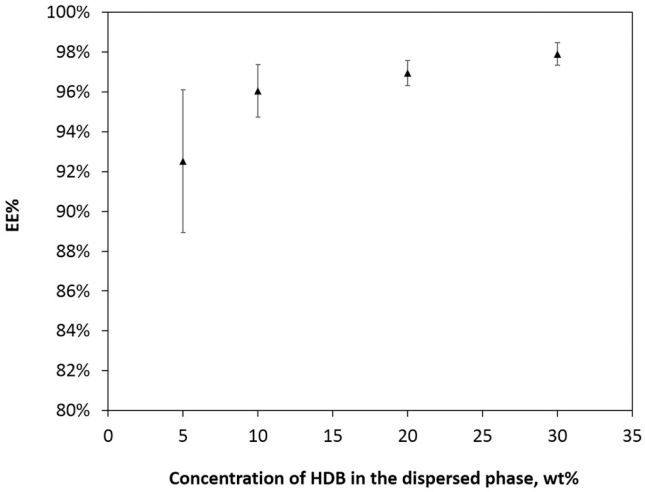

Fig. 11 – Encapsulation efficiency (EE %) of the microcapsules synthesized with different c_{HDB}. Size of the microcapsules: 78μm.

When the size of microcapsules is fixed at around 78 μm, the relationship between average EE % and different c_{HDB} (or shell thickness) is shown in Fig. 11. Overall, the EE % of microcapsules in this study is higher than 90%. Such high encapsulation efficiency is not surprising because the solubility of OS in the aqueous phase is very low (0.6206 *mg/L* at 25°C). During preparation of microcapsules, there are roughly 70–95 mg of OS in one litre of aqueous phase at 25°C. Hence, the theoretically EE % can be calculated as,

$$\frac{(70 - 0.62) \times 100\%}{70} = 99\% \quad (5)$$

when the c_{HDB} is 30 wt%. Although OS may not be all measured during extraction step due to the inadequate crushing of microcapsules, the measured EE % (98%) is very close to the theoretical one (99%) for the microcapsules fabricated with 30 wt% c_{HDB}. Besides, it can also be concluded that the diffusion of OS into the aqueous phase is faster than the formation of a polyurea shell.

The measured EE % decreases slightly with a decrease of c_{HDB} (or shell thickness). Moreover, the errors become more important when there is only 5 wt% HDB-LV in the droplet phase, as shown in Fig. 11. In fact, using less HDB-LV in the droplet phase results in more fragile shells of microcapsules.The SEM photos (Fig. 7d) show that after washing and drying these fragile microcapsules tend to stick together and even merge. After drying, the microcapsules produced with 5 wt% c_{HDB} form a pancake of microcapsules. To measure EE %, we have to cut a piece of this pancake to control the mass. Meanwhile, we observe that there is leakage of the OS during the cutting process. Besides, these microcapsules may also break during the drying process. Both phenomena above may lead to a lower measured EE % (93%) than the theoretical one (99%) for the microcapsules produced with 5 wt% c_{HDB}.

4. Discussion

4.1. *Importance of using a low amine concentration for the formation of spherical polyurea microcapsules*

In the presence of high c_{En} (1 wt%), the micrographs (Fig. 3) for the shape of microcapsules with different c_{HDB}, demonstrate that the spherical microcapsules can only be obtained with 5 wt% HDB-LV (Fig. 3b). And if c_{HDB} is over 5 wt %, c_{En} should be reduced to 0.01 wt% to avoid the deformation of microcapsules (Fig. 5).

In fact, the polyurea formation is a first-order reaction in each reactant (Yadav et al., 1990), which means the reaction rate is determined by both concentrations of amines and isocyanates. Therefore, the two phenomena above seem to reveal the same thing: to avoid the deformation of polyurea microcapsules, the concentrations of HDB-LV and En in the corresponding phases should not be so high simultaneously that the interfacial polymerization rate is too fast. The same phenomenon is also observed by (Ma et al., 2017) that the polyurea microcapsules are deformed because of a high reactivity and diffusivity of the En than other amines.

Why does a fast reaction rate lead to the deformation of the microcapsules? A hypothesis is given below:

1) Firstly, the fast solidification process may result in the loss of elasticity of formed droplets at beginning of the reaction, as illustrated in Fig. 4. Meanwhile, the formed polyurea shell may have uneven mechanic strength over the surface if the reaction rate is too fast.

2) After that, En molecules are more likely to enter through the fragile parts (defects) on the interface and continue to react with the HDB-LV at the defects or even inside the droplets. In fact, during interfacial polymerization, HDB-LV (big molecules) does not have enough time to transfer to the interface while En (small molecules) can diffuse rapidly into droplets.

3) Finally, this uneven cross-linking process leads to an uneven internal stress, which eventually causes the deformation of polyurea microcapsules.

To further verify our hypothesis, spherical and deformed microcapsules are cut carefully and characterized by the SEM. For both cases, the c_{HDB} is fixed at 30 wt%. Whereas the spherical one (Fig. 12a) corresponds to a c_{En} of 0.01 wt% and the deformed one (Fig. 12b) corresponds to a c_{En} of 1 wt%. From the evident net structure inside the deformed microcapsule, it can be concluded that a high amine concentration does lead to an internal cross-linking due to its fast diffusion and high reactivity. And this irregular cross-linking possibly results in the deformation of microcapsules because of the uneven internal stress.

Besides, this hypothesis explains also why the microcapsules fabricated with only 5 wt% of HDB-LV are all spherical (Fig. 3b) even under a high amine concentration (1 wt%). Though amine can still diffuse rapidly into droplets, there are much fewer HDB-LV molecules and thus the reaction slows down. So HDB-LV molecules can have enough time to transfer to the interface for the reaction.

Furthermore, when c_{En} is very low (0.01 wt%), the reaction rate is so slow that a polyurea shell with even mechanic strength is formed. The transfer of the En molecules through the interface is more even. Meanwhile, the droplets remain elastic for a long period of time because of the low reaction rate. Although it can create some craters on the surface of microcapsules, the formed microcapsules are globally spherical under a high concentration (30 wt%) of HDB-LV, as shown in Fig. 5a.

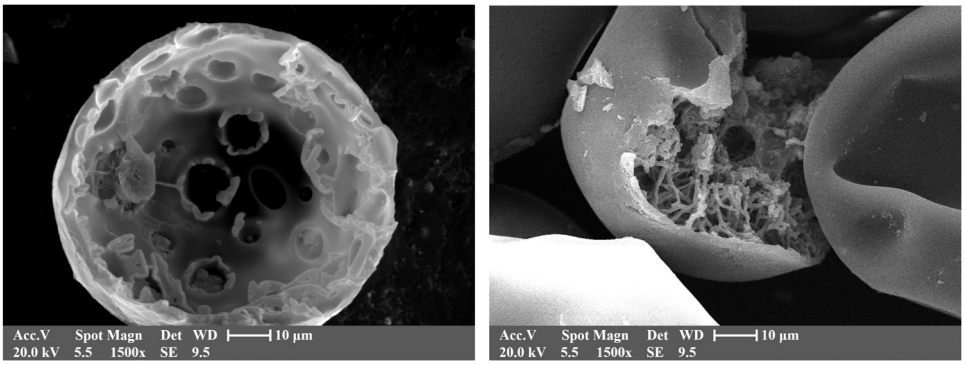

(a) (b)

Fig. 12 – SEM photos of two cut polyurea microcapsules fabricated with a c_{HDB} of 30 wt%. (a). The spherical one corresponds to a c_{En} of 0.01 wt%. (b). The deformed one corresponds to a c_{En} of 1 wt%.

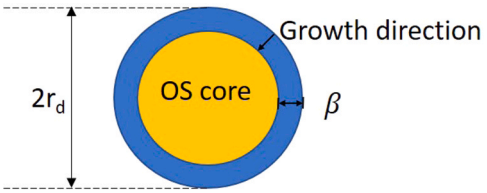

Fig. 13 – Schematic of a microcapsule for calculating the shell thickness.

Table 7 – The theoretical shell thickness (β_t) of the microcapsules synthesized with different c_{HDB}.

c_{HDB}, wt%, wt%	r_d, μm	β_t, μm
30	39	3.9
20	39	2.5
10	40	1.3
5	39	0.6

4.2. *A method for predicting shell thickness of the polyurea microcapsules*

For one microcapsule as illustrated in the Fig. 13, if the mass of a formed polyurea shell is known, then its thickness can be calculated through the mass balance equation as,

$$4\pi r_d^2 \beta \quad \rho_p = m_p \tag{6}$$

where m_p (kg) is the mass of a formed polyurea shell, r_d (m) is the radii of a droplet or the external radii of a microcapsule because polyurea grows towards inside a droplet, ρ_p (kg/m^3) is the density of polyurea and β (m) is the shell thickness. It should be noted that Eq. (6) is a simplified calculation of shell thickness for a β much smaller than r_d.

Then we have β as,

$$\beta = \frac{m_p}{4\pi r_d^2 \rho_p} \tag{7}$$

According to the reaction stoichiometry, m_p is the total mass of the reacted HDB-LV and En molecules in a microcapsule with a mass ratio of 1:0.17 as discussed in the Section 3.5.2. Then the m_p can be expressed as,

$$m_p = (1 + 0.17) \times \frac{4}{3}\pi r_d^3 \rho \quad c_{HDB} \tag{8}$$

where ρ is the density of dispersed phases and can be found from the supplementary material (Table S 2). Substituting the Eq. (8) into the Eq. (7), the shell thickness of a microcapsules is proportional to $r_d c_{HDB}$,

$$\beta = \frac{1.17 \times \frac{4}{3}\pi r_d^3 \rho \quad c_{HDB}}{4\pi r_d^2 \rho_p} = \frac{1.17 \times r_d \quad \rho \quad c_{HDB}}{3\rho_p} \tag{9}$$

So if the size of the droplets is fixed, a linear relationship between β and c_{HDB} should be obtained, and vice versa. The density of the polyurea is measured to be 1230 kg/m^3 by a pycnometer. The theoretical shell thickness (β_t) for all the microcapsules synthesized at different conditions are summarized in Table 7.

A comparison of theoretical and experimental results for the shell thickness of microcapsules are illustrated in Fig. 14. The factor between the theoretical and experimental shell thickness is calculated to be 1.5. This factor has two possible explanations: .

1) the actual density of the polyurea shell of the microcapsules is probably larger than the measured value (1230 kg/m^3) by a pycnometer. The measured volume of the polyurea samples may be larger than the actual volume because of the possible cavities inside if samples are not well compressed. Consequently, the measured density may be smaller than the actual one.

2) the volume of protrusions on the inner surface of microcapsules is not included in the Eq. (9). As shown in Fig. 12a for a cut microcapsule, there are lots of polyurea protrusions that are uniformly distributed on the inner surface of microcapsules. However, it is difficult to calculate the volume of these protrusions. In this study, we only choose the dense part (without any crater or protrusion) of the polyurea shell to measure its thickness.

Though there is a difference between the theoretical and experimental shell thickness, our experimental results still show a good linear relationship between β and c_{HDB} when the size of microcapsules is fixed. Nevertheless, our simple model divided with a factor of 1.5 can correctly reproduce the experimental results and can be used to predict the shell thickness of the microcapsules fabricated with different c_{HDB}. Moreover, it can be concluded that the density of the polyurea shell remains as constant, which is independent of the HDB-LV concentration in dispersed phases.

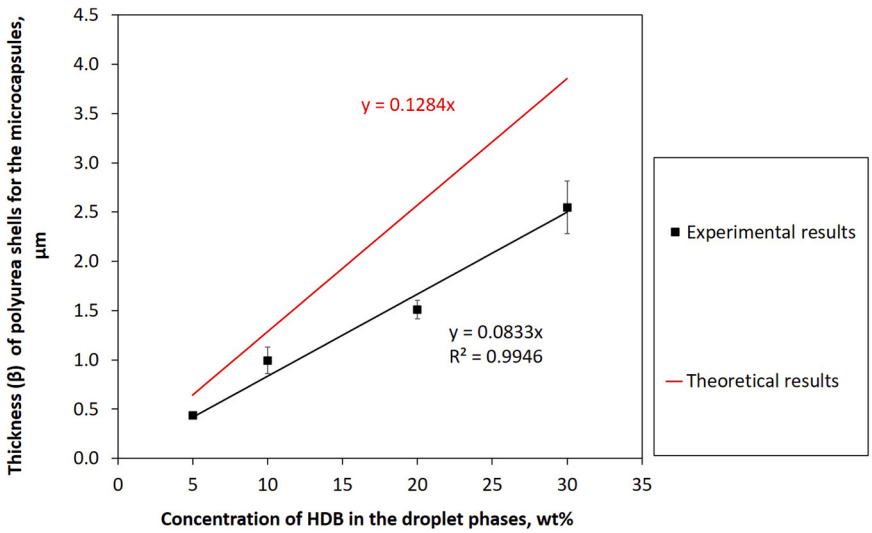

Fig. 14 – A comparison of the theoretical and experimental shell thickness at different c_{HDB}. Size of microcapsules: 78 μm.

5. Conclusion

In this study, spherical polyurea microcapsules are successfully synthesized when less toxic HDB-LV and octyl salicylate are used as the isocyanate and solvent respectively. High amine concentrations (> 0.01*wt*%) need to be avoided because they can cause the deformation of microcapsules. Except that, a solvent with relatively high solubility (dibutyl adipate) in the aqueous phase can cause failure of encapsulation because this solvent can diffuse into the outer phase during the polymerization step. Both experimental and theoretical results prove that the shell thickness of microcapsules increases linearly with the concentration of HDB-LV. High encapsulation efficiency (> 90%) for octyl salicylate is obtained for all the microcapsules.

Interestingly, this work has shown the influence of reaction and diffusion rates on the shape of microcapsules. These effects certainly deserve further work to look deeper into the mechanisms leading to this effect. One possibility would be to use other amines such as polyethylenimine and guanidine which are less reactive and can slow down reaction rates. Besides, it is necessary to determine the reaction kinetics of interfacial polymerization to evaluate the characteristic time of this reaction and compare it with that of the diffusion of monomers. A potential application of these microcapsules can be encapsulating PCM for thermal energy storage, such as the fabrication of outdoor clothing. For the next work, it may be necessary to test the mechanical resistance of the microcapsules.

Declaration of Competing Interest

The authors declare that they have no known competing financial interests or personal relationships that could have appeared to influence the work reported in this paper.

Appendix A. Supporting information

Supplementary data associated with this article can be found in the online version at doi:10.1016/j.cherd.2022.03.026.

References

Ahangaran, F., Navarchian, A., Picchioni, F., 2019. Material encapsulation in poly(methyl methacrylate) shell: A review. J. Appl. Polym. Sci. 136, 48039. https://doi.org/10.1002/app.48039

Alkan, C., Sari, A.S., Karaipekli, A., Uzun, O., 2009. Preparation, characterization, and thermal properties of microencapsulated phase change material for thermal energy storage. Sol. Energy Mater. Sol. Cells 93, 143–147. https://doi.org/10.1016/J.SOLMAT.2008.09.009

Arora, P., Jain, R., Mathur, K.M., Sharma, A.K., Gupta, A., 2010. Synthesis of polymethyl methacrylate ((pmma)) by batch emulsion polymerization.

Bulian, F., Graystone, J., 2009, Raw Materials for Wood Coatings (1) - Film Formers (Binders, Resins and Polymers).chapter 3. 53–94.10.1016/B978–0-444–52840-7.00003–5.

Cai, C., Ouyang, X., Zhou, L., Liu, G., Wang, Y., Zhu, G., Yao, J., Militky, J., Venkataraman, M., Zhang, G., 2020. Co-solvent free interfacial polycondensation and properties of polyurea pcm microcapsules with dodecanol dodecanoate as core material. Sol. Energy 199, 721–730. https://doi.org/10.1016/j.solener.2020.02.071

Chen, K., Zhou, J., Che, X., Zhao, R., Gao, Q., 2020. One-step synthesis of core shell cellulose-silica/n-octadecane microcapsules and their application in waterborne self-healing multiple protective fabric coatings. J. Colloid Interface Sci. 566, 401–410. https://doi.org/10.1016/j.jcis.2020.01.106

Chen, Z., Wang, J., Yu, F., Zhang, Z., Gao, X., 2015. Preparation and properties of graphene oxide-modified poly(melamine-formaldehyde) microcapsules containing phase change material n-dodecanol for thermal energy storage. J. Mater. Chem. A 3, 11624–11630. https://doi.org/10.1039/C5TA01852H

Cotting, F., Koebsch, A., Aoki, I.V., 2019. Epoxy self-healing coating by encapsulated epoxy ester resin in poly (urea-formaldehyde-melamine) microcapsules. Front. Mater. 6. https://doi.org/10.3389/fmats.2019.00314

De Castro, P.F., Shchukin, D.G., 2015. New polyurethane/docosane microcapsules as phase-change materials for thermal energy storage. Chem.-A Eur. J. 21, 11174–11179. https://doi.org/10.1002/chem.201500666

Di Credico, B., Griffini, G., Levi, M., Turni, S., 2013. Microencapsulation of a uv-responsive photochromic dye by means of novel uv-screening polyurea-based shells for smart coating applications. ACS Appl. Mater. Interfaces 5, 6628–6634. https://doi.org/10.1021/am401328f

Du, J., Ibaseta, N., Guichardon, P., 2020. Generation of an o/w emulsion in a flow-focusing microchip: Importance of wetting conditions and of dynamic interfacial tension. Chem. Eng.

Res. Des. 159, 615–627. https://doi.org/10.1016/j.cherd.2020.04.012
Eriksson, V., Andersson Trojer, M., Vavra, S., Hulander, M., Nordstierna, L., 2020. Formulation of polyphthalaldehyde microcapsules for immediate uv-light triggered release. J. Colloid Interface Sci. 579, 645–653. https://doi.org/10.1016/j.jcis.2020.06.024
Fei, X., Zhao, H., Zhang, B., Cao, L., Yu, M., Zhou, J., Yu, L., 2015. Microencapsulation mechanism and size control of fragrance microcapsules with melamine resin shell. Colloids Surf. A: Physicochem. Eng. Asp. 469, 300–306. https://doi.org/10.1016/j.colsurfa.2015.01.033
Fujiwara, M., Shoji, S., Murakami, Y., 2019. Controlled release of phosphate fertilizer using silica microcapsules. Chem. Lett. 48, 658–661. https://doi.org/10.1246/cl.190192
Fujiwara, S., Shoji, K., Watanabe, C., Kawano, R., Yanagisawa, M., 2020. Microfluidic formation of honeycomb-patterned droplets bounded by interface bilayers via bimodal molecular adsorption. Micromachines 11. https://doi.org/10.3390/mi11070701
Giro-Paloma, J., Alkan, C., Chimenos, J., Fernández, A., 2017. Comparison of microencapsulated phase change materials prepared at laboratory containing the same core and different shell material. Appl. Sci. 7, 723. https://doi.org/10.3390/app7070723
He, R.H., Wang, J.P., Wang, X.C., Li, W., Zhang, X.X., 2018. Fabrication and characterization of core-shell novel pu microcapsule using tdi trimer for release system. Colloids Surf. A-Phys. Eng. Asp. 550, 138–144. https://doi.org/10.1016/j.colsurfa.2018.03.071
He, Y., Yao, S., Hao, J., Wang, H., Zhu, L., Si, T., Sun, Y., Lin, J., 2019. Synthesis of melamine-formaldehyde microcapsules containing oil-based fragrances via intermediate polyacrylate bridging layers. Chin. J. Chem. Eng. 27, 2574–2580. https://doi.org/10.1016/j.cjche.2018.10.023
Hedaoo, R.K., Mahulikar, P.P., Chaudhari, A.B., Rajput, S.D., Gite, V.V., 2014. Fabrication of core-shell novel polyurea microcapsules using isophorone diisocyanate (ipdi) trimer for release system. Int. J. Polym. Mater. Polym. Biomater. 63, 352–360. https://doi.org/10.1080/00914037.2013.845191
Huang, M., Yang, J., 2011. Facile microencapsulation of hdi for self-healing anticorrosion coatings. J. Mater. Chem. 21, 11123–11130. https://doi.org/10.1039/C1JM10794A
Ina, M., Zhushma, A.P., Lebedeva, N.V., Vatankhah-Varnoosfaderani, M., Olson, S.D., Sheiko, S.S., 2016. The design of wrinkled microcapsules for enhancement of release rate. J. Colloid Interface Sci. 478, 296–302. https://doi.org/10.1016/j.jcis.2016.06.022
Jacquemond, M., Jeckelmann, N., Ouali, L., Haefliger, O.P., 2009. Perfume-containing polyurea microcapsules with undetectable levels of free isocyanates. J. Appl. Polym. Sci. 114, 3074–3080. https://doi.org/10.1002/app.30857
Jerri, H.A., Jacquemond, M., Hansen, C., Ouali, L., Erni, P., 2016. “suction caps”: Designing anisotropic core/shell microcapsules with controlled membrane mechanics and substrate affinity. Adv. Funct. Mater. 26, 6224–6237. https://doi.org/10.1002/adfm.201601563
Ji, H., Long, Q., He, Y., Yao, X., 2010. Palladium nanoclusters entrapped in polyurea: A recyclable and efficient catalyst for reduction of nitro-benzenes and hydrodechlorination of halogeno-benzenes. Sci. China Chem. 53, 1520–1524. https://doi.org/10.1007/s11426-010-4027-7
Ji, X.P., Li, J., Hua, W.L., Hu, Y.L., Si, B.T., Chen, B., 2021. Preparation and performance of microcapsules for asphalt pavements using interfacial polymerization. Constr. Build. Mater. 289. https://doi.org/10.1016/j.conbuildmat.2021.123179
Jialan, Y., Chenpeng, Y., Chengfei, Z., Baoqing, H., 2019. Preparation process of epoxy resin microcapsules for self-healing coatings. Progress Organic Coatings 132, 440–444. https://doi.org/10.1016/j.porgcoat.2019.04.015
Khun, N.W., Sun, D.W., Huang, M.X., Yang, J.L., Yue, C.Y., 2014. Wear resistant epoxy composites with diisocyanate-based self-healing functionality. Wear 313, 19–28. https://doi.org/10.1016/j.wear.2014.02.011
Kim, J.C., Song, M.E., Lee, E.J., Park, S.k., Rang, M.J., Ahn, H.J., 2001. Preparation and characterization of triclosan-containing microcapsules by complex coacervation. J. Dispersion Sci. Technol. 22, 591–596. https://doi.org/10.1081/DIS-100107758
Lai, S., He, Y., Xiong, D., Wang, Y., Xiao, K., Yan, Z., Zhang, H., 2021. Fabrication and property regulation of small-size polyamine microcapsules via integrating microfluidic t-junction and interfacial polymerization. Materials 14. https://doi.org/10.3390/ma14071800
Lei, C., Li, Q., Yang, L., Deng, F., Li, J., Ye, Z., Wang, Y., Zhang, Z., 2019. Controlled reversible buckling of polydopamine spherical microcapsules: revealing the hidden rich phenomena of post-buckling of spherical polymeric shells. Soft Matter 15, 6504–6517. https://doi.org/10.1039/C9SM00705A
León, G., Paret, N., Fankhauser, P., Grenno, D., Erni, P., Ouali, L., Berthier, D.L., 2017. Formaldehyde-free melamine microcapsules as core/shell delivery systems for encapsulation of volatile active ingredients. RSC Adv 7, 18962–18975. https://doi.org/10.1039/C7RA01413A
Li, H., Feng, Y., Cui, Y., Ma, Y., Zheng, Z., Qian, B., Wang, H., Semenov, A., Shchukin, D., 2020. Polyurea/polyaniline hybrid shell microcapsules loaded with isophorone diisocyanate for synergetic self-healing coatings. Progress Organic Coatings 145, 105684. https://doi.org/10.1016/j.porgcoat.2020.105684
Liu, L., Yang, J.P., Ju, X.J., Xie, R., Yang, L., Liang, B., Chu, L.Y., 2009. Microfluidic preparation of monodisperse ethyl cellulose hollow microcapsules with non-toxic solvent. J. Colloid Interface Sci. 336, 100–106. https://doi.org/10.1016/j.jcis.2009.03.050
Liu, Y., Zheng, J., Zhang, X., Du, Y., Li, K., Yu, G., Jia, Y., Zhang, Y., 2021. Mussel-inspired and aromatic disulfide-mediated polyurea-urethane with rapid self-healing performance and water-resistance. J. Colloid Interface Sci. 593, 105–115. https://doi.org/10.1016/j.jcis.2021.03.003
Lone, S., Lee, H.M., Kim, G.M., Koh, W.G., Cheong, I.W., 2013. Facile and highly efficient microencapsulation of a phase change material using tubular microfluidics. Colloids Surf. A: Phys. Eng. Asp. 422, 61–67. https://doi.org/10.1016/j.colsurfa.2013.01.035
Lu, S., Xing, J., Zhang, Z., Jia, G., 2011. Preparation and characterization of polyurea/polyurethane double-shell microcapsules containing butyl stearate through interfacial polymerization. J. Appl. Polym. Sci. 121, 3377–3383. https://doi.org/10.1002/app.33994
Lu, S.F., Shen, T.W., Xing, J.W., Song, Q.W., Xin, C., 2017. Preparation, characterization, and thermal stability of double-composition shell microencapsulated phase change material by interfacial polymerization. Colloid Polym. Sci. 295, 2061–2067. https://doi.org/10.1007/s00396-017-4189-3
Luo, Z., Zhao, G., Panhwar, F., Akbar, M.F., Shu, Z., 2017. Well-designed microcapsules fabricated using droplet-based microfluidic technique for controlled drug release. J. Drug Deliv. Sci. Technol. 39, 379–384. https://doi.org/10.1016/j.jddst.2017.04.016
Ma, Y., Chu, X., Tang, G., Yao, Y., 2012. Adjusting phase change temperature of microcapsules by regulating their core compositions. Mater. Lett. 82, 39–41. https://doi.org/10.1016/j.matlet.2012.05.033
Ma, Y., Jiang, Y., Tan, H., Zhang, Y., Gu, J., 2017. A rapid and efficient route to preparation of isocyanate microcapsules. Polymers 9. https://doi.org/10.3390/polym9070274
Matamoros-Ambrocio, M., SánchezMora, E., Gómez-Barojas, E., López, J., 2021. Synthesis and study of the optical properties of pmma microspheres and opals. Polymers 13, 2171. https://doi.org/10.3390/polym13132171
Muneratto, V.M., Gallo, T.C.B., Nicoletti, V.R., 2021. Oregano essential oil encapsulation following the complex coacervation method: Influence of temperature, ionic strength, and ph on the release kinetics in aqueous medium. Ciência e Agrotecnol. 45. https://doi.org/10.1590/1413-7054202145003221

Nandiyanto, A.B.D., Suhendi, A., Ogi, T., Iwaki, T., Okuyama, K., 2012. Synthesis of additive-free cationic polystyrene particles with controllable size for hollow template applications. Colloids Surf. A: Phys. Eng. Asp. 396, 96–105. https://doi.org/10.1016/j.colsurfa.2011.12.048

Nguon, O., Lagugné-Labarthet, F., Brandys, F.A., Li, J., Gillies, E.R., 2018. Microencapsulation by in situ polymerization of amino resins. Polym. Rev. 58, 326–326–375. https://doi.org/10.1080/15583724.2017.1364765

Njoku, C.N., Bai, W., Arukalam, I.O., Yang, L., Hou, B., Njoku, D.I., Li, Y., 2020. Epoxy-based smart coating with self-repairing polyurea-formaldehyde microcapsules for anticorrosion protection of aluminum alloy aa2024. J. Coat. Technol. Res. 17, 797–813. https://doi.org/10.1007/s11998-020-00334-3

Onder, E., Sarier, N., Cimen, E., 2008. Encapsulation of phase change materials by complex coacervation to improve thermal performance of woven fabrics. Thermochim. Acta 467, 63–72. https://doi.org/10.1016/j.tca.2007.11.007

Park, S., Cho, Y.A., Park, S., Oh, M., Kim, D., Lim, G., Park, J.J., 2019. Polyurea microcapsules with different phase change material for thermochromic smart displays. Chem. Lett. 48, 1343–1346. https://doi.org/10.1246/cl.190629

Pascu, O., Garcia-Valls, R., Giamberini, M., 2008. Interfacial polymerization of an epoxy resin and carboxylic acid for the synthesis of microcapsules. Polym. Int. 57, 995–1006. https://doi.org/10.1002/pi.2438

Perez, A., Hernández, R., Velasco, D., Voicu, D., Mijangos, C., 2015. Poly (lactic-co-glycolic acid) particles prepared by microfluidics and conventional methods. modulated particle size and rheology. J. Colloid Interface Sci. 441, 90–97. https://doi.org/10.1016/j.jcis.2014.10.049

Polenz, I., Datta, S.S., Weitz, D.A., 2014. Controlling the morphology of polyurea microcapsules using microfluidics. Langmuir 30, 13405–13410. https://doi.org/10.1021/la503234z

Polenz, I., Weitz, D.A., Baret, J.C., 2015. Polyurea microcapsules in microfluidics: surfactant control of soft membranes. Langmuir 31, 1127–1134. https://doi.org/10.1021/la5040189

Raeesi, M., Mirabedini, S.M., Farnood, R.R., 2017. Preparation of microcapsules containing benzoyl peroxide initiator with gelatin-gum arabic/polyurea-formaldehyde shell and evaluating their storage stability. ACS Appl. Mater. Interfaces 9, 20818–20825. https://doi.org/10.1021/acsami.7b03708

Sarí, A., Alkan, C., Karaipekli, A., 2010. Preparation, characterization and thermal properties of pmma/n-heptadecane microcapsules as novel solid-liquid micropcm for thermal energy storage. Appl. Energy 87, 1529–1534. https://doi.org/10.1016/j.apenergy.2009.10.011

Sari, A., Alkan, C., Karaipekli, A., Uzun, O., 2009. Microencapsulated n-octacosane as phase change material for thermal energy storage. Sol. Energy 83. https://doi.org/10.1016/J.SOLENER.2009.05.008

Scarfato, P., Avallone, E., Iannelli, P., De Feo, V., Acierno, D., 2007. Synthesis and characterization of polyurea microcapsules containing essential oils with antigerminative activity. J. Appl. Polym. Sci. 105, 3568–3577. https://doi.org/10.1002/app.26420

Shaddel, R., Hesari, J., Azadmard-Damirchi, S., Hamishehkar, H., Fathi-Achachlouei, B., Huang, Q., 2018. Use of gelatin and gum arabic for encapsulation of black raspberry anthocyanins by complex coacervation. Int. J. Biol. Macromol. 107, 1800–1810. https://doi.org/10.1016/j.ijbiomac.2017.10.044

Shi, T.J., Hu, P., Wang, J.T., 2020. Preparation of polyurea microcapsules containing phase change materials using microfluidics. Chemistryselect 5, 2342–2347. https://doi.org/10.1002/slct.201904570

Sánchez-Silva, L., Lopez, V., Cuenca, N., Valverde, J.L., 2018. Poly (urea-formaldehyde) microcapsules containing commercial paraffin: in situ polymerization study. Colloid Polym. Sci. 296, 1449–1457. https://doi.org/10.1007/s00396-018-4365-0

Sui, C., Preece, J.A., Zhang, Z.B., Yu, S.H., 2021. Efficient encapsulation of water soluble inorganic and organic actives in melamine formaldehyde based microcapsules for control release into an aqueous environment. Chem. Eng. Sci. 229. https://doi.org/10.1016/j.ces.2020.116103

Sun, D., An, J., Wu, G., Yang, J., 2015. Double-layered reactive microcapsules with excellent thermal and non-polar solvent resistance for self-healing coatings. J. Mater. Chem. A 3, 4435–4444. https://doi.org/10.1039/C4TA05339G

Sun, S., Gao, Y., Han, N., Zhang, X., Li, W., 2021. Reversible photochromic energy storage polyurea microcapsules via in-situ polymerization. Energy 219, 119630. https://doi.org/10.1016/j.energy.2020.119630

Sun, Y., Wang, R., Liu, X., Dai, E., Li, B., Fang, S., Li, D., 2018. Synthesis and performances of phase change microcapsules with a polymer/diatomite hybrid shell for thermal energy storage. Polymers 10. https://doi.org/10.3390/polym10060601

Takahashi, T., Taguchi, Y., Tanaka, M., 2007. Shell thickness and chemical structure of polyurea microcapsules prepared with haxamethylene diisocyanate uretidione and isocyanurate. J. Appl. Polym. Sci. 106, 3786–3791. https://doi.org/10.1002/app.25061

Tian, Q., Zhou, W., Cai, Q., Ma, G., Lian, G., 2021. Concepts, processing, and recent developments in encapsulating essential oils. Chin. J. Chem. Eng. 30, 255–271. https://doi.org/10.1016/j.cjche.2020.12.010

Tzavidi, S., Zotiadis, C., Porfyris, A., Korres, D.M., Vouyiouka, S., 2020. Epoxy loaded poly(urea-formaldehyde) microcapsules via in situ polymerization designated for self-healing coatings. J. Appl. Polym. Sci. 137, 49323. https://doi.org/10.1002/app.49323

Valerie Jeanne-Rose, Y.R., 2007. Composite dyestuff of microcapsule type and cosmetic use thereof, 1837073.

Wang, H.R., Zhou, Q.X., 2018. Evaluation and failure analysis of linseed oil encapsulated self-healing anticorrosive coating. Progress Organic Coat. 118, 108–115. https://doi.org/10.1016/j.porgcoat.2018.01.024

Wang, S., Zhang, W., Chen, Y.F., Zhang, S.L., Wang, W., 2019. The aromatic properties of polyurea-encapsulated lavender oil microcapsule and their application in cotton fabrics. J. Nanosci. Nanotechnol. 19, 4147–4153. https://doi.org/10.1166/jnn.2019.16334

Wu, K., Chen, Y., Luo, J., Liu, R., Sun, G., Liu, X., 2021. Preparation of dual-chamber microcapsule by pickering emulsion for self-healing application with ultra-high healing efficiency. J. Colloid Interface Sci. 600, 660–669. https://doi.org/10.1016/j.jcis.2021.05.066

Yadav, S.K., Suresh, A.K., Khilar, K.C., 1990. Microencapsulation in polyurea shell by interfacial polycondensation. AIChE J. 36, 431–438. https://doi.org/10.1002/aic.690360312

Yang, Y., Wei, Z., Wang, C., Tong, Z., 2013. Versatile fabrication of nanocomposite microcapsules with controlled shell thickness and low permeability. ACS Appl. Mater. Interfaces 5, 2495–2502. https://doi.org/10.1021/am302963d

Yang, Y., Ye, X., Luo, J., Song, G., Liu, Y., Tang, G., 2015. Polymethyl methacrylate based phase change microencapsulation for solar energy storage with silicon nitride. Sol. Energy 115, 289–296. https://doi.org/10.1016/j.solener.2015.02.036

Yang, Z., Fang, X., Peng, J., Cao, X., Liao, Z., Yan, Z., Jiang, C., Liu, B., Zhang, H., 2020. Versatility of the microencapsulation technique via integrating microfluidic t-junction and interfacial polymerization in encapsulating different polyamines. Colloids Surf. A: Physicochem. Eng. Asp. 604, 125097. https://doi.org/10.1016/j.colsurfa.2020.125097

Yun, H.R., Li, C.L., Zhang, X.X., 2019. Fabrication and characterization of conductive microcapsule containing phase change material. e-Polymers 19, 519–526. https://doi.org/10.1515/epoly-2019-0055

Zhang, B., Li, S., Fei, X., Zhao, H., Lou, X., 2020. Enhanced mechanical properties and thermal conductivity of paraffin microcapsules shelled by hydrophobic-silicon carbide modified melamine-

formaldehyde resin. Colloids Surf. A: Physicochem. Eng. Asp. 603, 125219. https://doi.org/10.1016/j.colsurfa.2020.125219
Zhang, H., Zhang, X., Chong, Y.B., Peng, J., Fang, X., Yan, Z., Liu, B., Yang, J., 2019a. Shell formation mechanism for direct microencapsulation of nonequilibrium pure polyamine droplet. J. Phys. Chem. C 123, 22413–22423. https://doi.org/10.1021/acs.jpcc.9b06544
Zhang, W.X., Qu, L.L., Pei, H., Qin, Z., Didier, J., Wu, Z.W., Bobe, F., Ingber, D.E., Weitz, D.A., 2019b. Controllable fabrication of inhomogeneous microcapsules for triggered release by osmotic pressure. SMALL 15. https://doi.org/10.1002/smll.201903087
Zhang, X., Luo, J., Zhang, D., Jing, T., Li, B., Liu, F., 2018. Porous microcapsules with tunable pore sizes provide easily controllable release and bioactivity. J. Colloid Interface Sci. 517, 86–92. https://doi.org/10.1016/j.jcis.2018.01.100
Zhang, Y., Rochefort, D., 2012. Characterisation and applications of microcapsules obtained by interfacial polycondensation. J. Microencapsul 29, 636–649. https://doi.org/10.3109/02652048.2012.676092